ORIGINAL ARTICLE

Sacrospinous and sacrotuberous ligaments influence in pelvis kinematics

Petr Henyš[1] | Maziar Ramezani[2] | Daniel Schewitz[2] | Andreas Höch[3] |
Dustin Möbius[4] | Benjamin Ondruschka[4] | Niels Hammer[3,5,6]

[1]Institute of New Technologies and Applied Informatics, Faculty of Mechatronics, Informatics and Interdisciplinary Studies, Technical University of Liberec, Liberec, Czech Republic

[2]Department of Mechanical Engineering, Auckland University of Technology, Auckland, New Zealand

[3]Department of Trauma, Orthopedic and Plastic Surgery, University Hospital of Leipzig, Leipzig, Germany

[4]Institute of Legal Medicine, University Medical Centre Hamburg-Eppendorf, Hamburg, Germany

[5]Division of Macroscopic and Clinical Anatomy, Gottfried Schatz Research Center, Medical University of Graz, Graz, Austria

[6]Fraunhofer Institute for Machine Tools and Forming Technology, Dresden, Germany

Correspondence
Niels Hammer, Division of Macroscopic and Clinical Anatomy, Gottfried Schatz Research Center, Medical University of Graz, Harrachgasse 21/1, Graz, Austria.
Email: niels.hammer@medunigraz.at

Abstract

The alteration in mechanical properties of posterior pelvis ligaments may cause a biased pelvis deformation which, in turn, may contribute to hip and spine instability and malfunction. Here, the effect of different mechanical properties of ligaments on lumbopelvic deformation is analyzed via the finite element method. First, the improved finite element model was validated using experimental data from previous studies and then used to calculate the sensitivity of lumbopelvic deformation to changes in ligament mechanical properties, load magnitude, and unilateral ligament resection. The deformation of the lumbopelvic complex relative to a given load was predominant in the medial plane. The effect of unilateral resection on deformation appeared to be counterintuitive, suggesting that ligaments have the ability to redistribute load and that they play an important role in the mechanics of the lumbopelvic complex.

KEYWORDS
elasticity, finite element method, hip–spine syndrome, lumbopelvic transition, pelvic ligaments, sacroiliac joint

1 | INTRODUCTION

The sacrotuberous ligament (ST) has gained increasing interest over the last years as an entrapment site for the pudendal nerve syndrome requiring surgery (Bollens et al., 2021; Kaur & Singh, 2022; Ploteau et al., 2016). Similarly, the ST ligament seems to play a role in hamstring injury (Bierry et al., 2014). It has gained attention as an attachment site for pelvic organ prolapse (De Decker et al., 2020).

Owing to their complex geometry, sparse data are available on the fine anatomy and mechanical properties of the posterior pelvis ligaments. The sacrospinous (SS) and ST ligaments are derived from involuted tail muscles. Muscle fibers are observed in the SS ligament for the first two to three decades of life (Hayashi et al., 2013). Connections of the SS ligament extend to the pelvic floor, falciform process, internal obturator fascia, and likely to the muscles of the urogenital diaphragm. The ST ligament is proximally interwoven with the long posterior sacroiliac ligament, the sacral origin of the gluteus maximus, and forms a further site of origin of the hamstring muscles. Both ligaments form a joint complex situated at the posterior pelvis. They connect the sacral ala with

bony prominences of the ischium. While proximally at the sacrum, their combined origin mainly comprises densely interwoven type 1 collagens (Fick, 1904; Hayashi et al., 2013), the SS ligament is formed anteriorly-superiorly to insert at the ischial spine. The ST ligament traverses posteriorly-inferiorly relative to the SS ligament and fans out to insert at the ischial tuberosity. The geometry of the smaller SS ligament is distorted by the twisting fibers, thereby forming a frustum (Hammer et al., 2009). Similarly, the larger ST ligament is formed by two combined frustums (bifrustum), with an opposite twist when compared to the SS ligament on the same side (Hammer et al., 2009). This opposite twist causes an area of minimal cross section approximately half way the length of the ligament, and potentially a prestrain to the posterior pelvis. Between both structures, an opening is formed at the posterior pelvis, the lesser sciatic foramen, which permits passage of the (pudendal) neurovascular bundle supplying the pelvic floor (Fick, 1904; Hayashi et al., 2013).

The ligaments have to date sparsely been investigated biomechanically in spite of their relevance in pelvis kinematics (Aldabe et al., 2019; Böhme et al., 2011, 2014; Hammer, Scholze, et al., 2019; Hammer et al., 2013) with related surgery, and yet their function remains unelucidated. Such findings would help inform clinical practice on surgical treatment of both pelvic injury and pudendal nerve entrapment (Philippeau et al., 2008) and potentially hamstring injury. Sparse data exist on the material properties and the underlying structural features of both ligaments, which likely causes a bias, especially in numerical studies where the ligaments are attributed estimates of uniaxial material properties derived indirectly from other anatomical regions. Owing to this uncertainty, to date, little reliable information can be given on the kinematic effects of surgical ligament transection for nerve entrapment therapy or pelvic injury.

The aim of this given numerical study was to assess the influence of three different configurations for the SS and ST ligaments on pelvis kinematics. For this purpose, a detailed and previously validated model of the osteoligamentous pelvis was used (Hammer, Scholze, et al., 2019; Ramezani et al., 2019), which has been extended to include the hip joint to allow for a more realistic motion of the sacrum relative to a movable innominate bone. It has been hypothesized that (A) lowering material stiffness for the SS and ST ligaments improves the accuracy of in silico with in vitro kinematics for the osteoligamentous pelvis. Moreover, it has been hypothesized that (B) complete transection of the SS and ST ligaments alters deformation patterns and load response of the pelvis when compared to the intact state.

The results of the computer model were compared with experimental results from the authors' previous study (Hammer, Scholze, et al., 2019; Ramezani et al., 2019). In addition, a sensitivity analysis of the pelvic deformation with respect to the load from the upper body was performed using the finite element (FE) method. The purpose of this sensitivity analysis was to identify significant pelvic deformations and understand their significance in the kinematics of the pelvic region.

2 | MATERIALS AND METHODS

A FE model of a pelvis previously developed and refined (Ramezani et al., 2019; Toyohara et al., 2020; Venayre et al., 2021) was deployed to analyze the deformation of the pelvis as a response to different load force representing upper body part and different elastic properties of the SS and ST ligaments. Bone geometries were extracted from the computed tomography scan of a healthy male (29 years, body height 185 cm, body weight 69 kg). The scanner used was a Somatom® Volume Zoom Scanner (Siemens AG). The slice thickness was 0.5 mm. The segmentation was done using Amira 3.1.1 (VSG). The triangulated surfaces of bones segmented were converted to CAD by approximating with NURBS patches in software Geomagic studio (Morrisville, NC, USA). The resultant assembly was imported to FE software Ansys (ANSYS, Inc.). The bone assembly was meshed by tetrahedral elements (141,672 tetrahedral elements, which roughly corresponded to element sizes ranging from 1 to 5 mm).

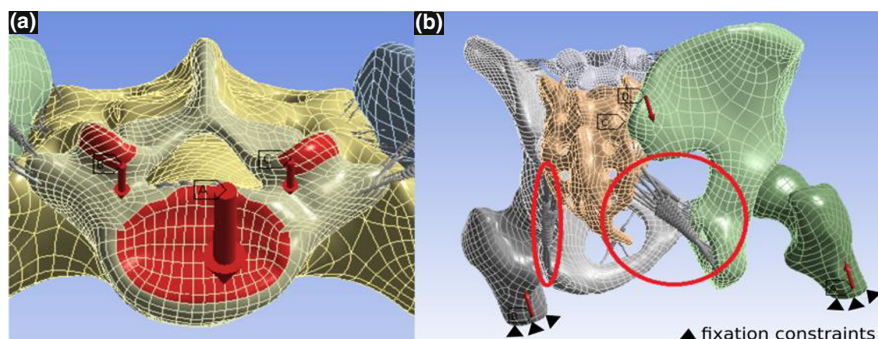The boundary conditions in the FE model are shown in Figure 1.

FIGURE 1 The finite element model of a male pelvis with boundary conditions applied and the sacrospinous and sacrotuberous ligaments is shown. (a) Cranial view of the posterior pelvis, showing the L5 endplate and facet joints (red areas) being loaded superior-inferiorly (red arrows), (b) posterior–lateral view of the right aspect of the pelvis (red ellipses indicate the sacrospinous-sacrotuberous complex on both sides).

Both femora (central shaft region) were fully constrained. A "glued" type contact was considered between the bone and cartilage contact surfaces, which does not allow relative movement of the surfaces. (Ramezani et al., 2019; Sichting et al., 2014) The element quality metric was defined according to Ansys software (a function of element volume and edge length). The mean value over all elements of this metric was 0.75 (0—bad, 1—best). A load force of 500 N was applied to the endplate of the L5 vertebra aligned with an axis directed superior-inferiorly along the axis of the lumbosacral transition and sacrum. The cortical shell measured 2 mm in thickness and was constant for all bones and sites (Ramezani et al., 2019). The ligaments were represented by linear springs with the stiffness defined as $k = E \times A/L$. "E" was defined as the modulus of elasticity, "A" as the cross-sectional area, and "L" as the length of the ligament. For the ligaments of the hip capsule, the following material properties were assigned in line with own previous experiments (Schleifenbaum et al., 2016): the iliofemoral ligament had an elastic modulus of 24 MPa, the ischiofemoral ligament 22 MPa, and the pubofemoral ligament 25 MPa. Static analysis was performed with different configurations in material

properties of SS/ST ligaments (see Table 1). The Poisson's ratio was kept constant at 0.3.

The first configuration "Stiffer state" considers the elastic properties of both ligaments to equal a value of 25 MPa, while the second configuration "Soft state" integrated the elastic properties of the ligaments based on previous authors' experiments considering the decreased mechanical stiffness of the SS and ST when compared to the sacroiliac ligaments (Böhme et al., 2011; Hülse et al., 2009). For the third configuration, "Transected state", the complex of SS and ST was "transected" unilaterally as done in surgery, for example, for pudendal nerve release.

Additionally, the load force was varied to check the sensitivity of pelvis deformation to trunk load. Force was varied in a range of 100–500 N in 100 N-steps according to cadaveric experiments of the authors (Hammer, Scholze, et al., 2019). The stiffness was given by a force applied and deformation at locations described in Figure 2. Therefore, the displacement and rotation vectors were computed with the FE method.

Points where the deformations were measured are shown in Figure 2. Those points were previously shown to be good indicators of pelvis ring deformation and stability and served as validation points in computer-cadaveric studies (Hammer, Scholze, et al., 2019; Ramezani et al., 2019). Point S_M was defined in the ventral center of the sacrum or the left (S_L). The point I represented two locations at the innominate bones (I_1, I_2). Points P were positioned in the area of the superior pubic ramus, in proximity to the pubic symphysis, and were distinguished for side, that is, P_L and P_R. Point L was allocated at the center of the fifth lumbar vertebra (L_5).

2.1 | Sensitivity of deformation to load

The relation of load force and displacements/rotations was found to be approximately linear, though the FE model considered the
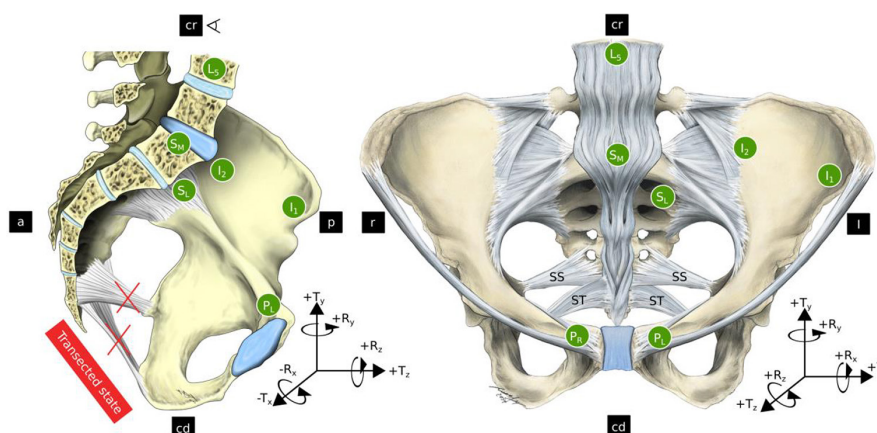
TABLE 1 The three configurations of different elastic modulus values for the sacrospinous (SS) and sacrotuberous (ST) ligaments tested

State	Stiffer	Soft	Transected
	SS & ST with the same stiffness as sacroiliac ligaments	SS & ST material properties derived from Hülse et al. (2009)	SS & ST completely transected on the left side (right side: 25/25)
E of SS/ST (MPa)	25/25	6.7/20.1	0/0

FIGURE 2 Locations of anatomical points, their directions of translations T, and rotations R within the coordinate system from an anterior–posterior (right image) and medial–lateral view (left image); a, anterior; cd, caudal; cr, cranial; l, left; p, posterior; r, right. Sacroiliac joint, movement of the sacrum (S_L) relative to the ilium (I_1); Lumbosacral transition, movement of the fifth lumbar vertebra (L_5) relative to the sacrum (S_M). Innominate bone, movement of the pubis (P_L) relative to the ilium (I_2); Pubic symphysis, movement of the left relative to the right superior pubic ramus (P_R-P_L), according to Hammer, Scholze, et al. (2019).

potential effects of large deformations. Hence, the slope value from linear regression was deemed sufficient to analyze the sensitivity of deformation (displacements/rotations) to the load force. The higher the value, the more sensitive the deformation is to the load, regardless of the sign. A negative value indicates that the deformation is inversely proportional to the magnitude of the load, whereas a positive value indicates a direct proportionality between the deformation and the magnitude of the load.

2.2 | Differences in ligament elasticity

For the comparison between the configurations ("Stiffer state", "Soft state" and "Transected state"), the absolute deformations of the abovementioned points as well as the relative deformations between the selected pairs of points according to the experimental study (Hammer, Scholze, et al., 2019; Ramezani et al., 2019) were considered. The differences between the configurations were expressed as a relative percentage difference for the two sets of deformations.

2.3 | Computer model validation and accuracy

The validity and accuracy of the computer model was analyzed visually on the dependence of deformation and load force. The curves of the mean values and standard deviation were calculated from the experimental data obtained from previous studies.

Subsequently, the level of overlap between the experimental results and the FE model results was analyzed qualitatively.

3 | RESULTS

3.1 | Computer model validation

The computed relative displacements T_x overlap the experimental displacements specifically for groups L_5-S_M and P_R-P_L, while the displacements for T_y for all computational groups overlapped with the cadaveric experiments. Figure 3 summarizes graphically the comparison of the computational and experimental relative displacements and rotations. Computed displacement T_z was within the experimental range of groups L_5-S_M and P_R-P_L, but not in I_1-S_L or P_L-I_2. Computed rotation R_x was in the experimental range only for group P_R-P_L. The rotation R_y was in the experimental range for the regions L_5-S_M and P_L-I_2. The computed rotation R_z lies in the experimental range of all groups except P_R-P_L.

3.2 | Absolute deformation sensitivity

The highest displacement sensitivity of value $-1.58\,\mu m/N$ was found for the displacement of L_5 in the axis-y. In contrast, the lowest value $-0.003\,\mu m/N$ was found for point I_1 in axis-x, as depicted in Figure 4. The highest rotation sensitivity of value 0.66 millidegree/N was found for L_5 around the axis-x, while the lowest
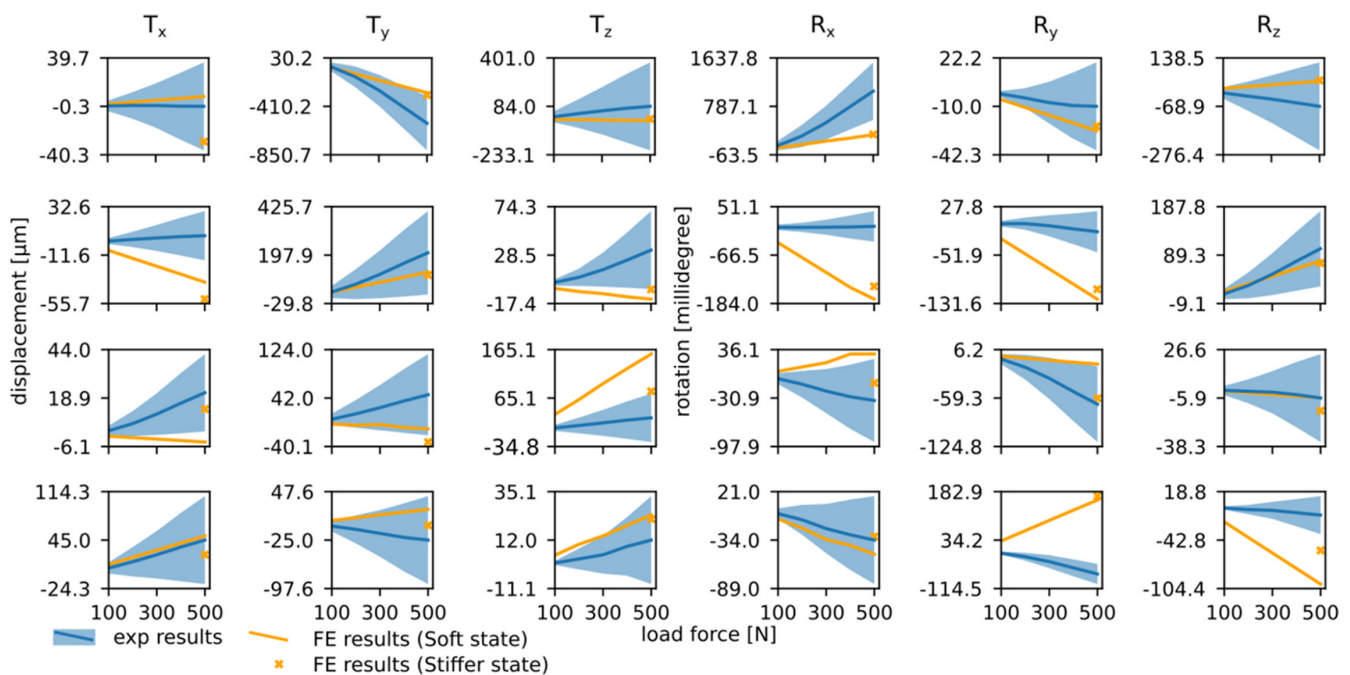

FIGURE 3 Comparison of experimental and computational results ("Soft state") for relative displacements T (micrometers) and rotations R (millidegrees). The blue area represents mean values ± standard deviation. The orange cross represents results at 500-N load in the stiff FE model ("Stiffer state").
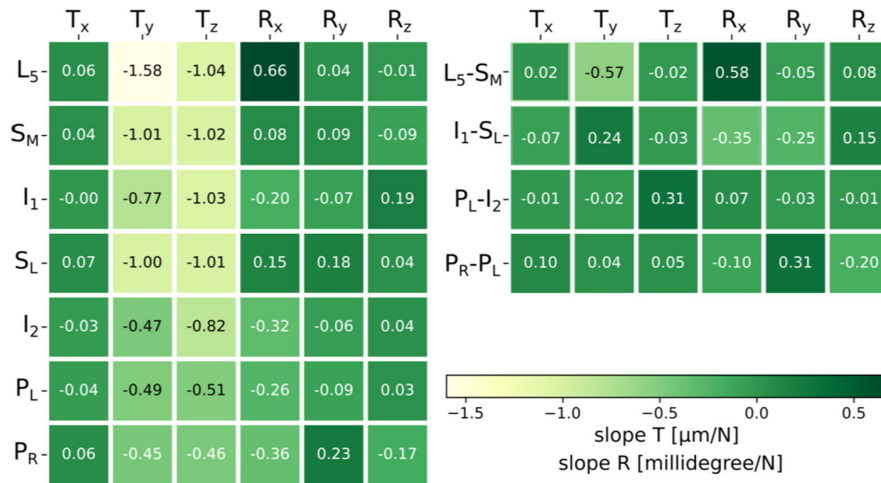
FIGURE 4 The sensitivity (slope) of absolute and relative displacements and rotations to loading forces computed with finite elements model "Soft state".
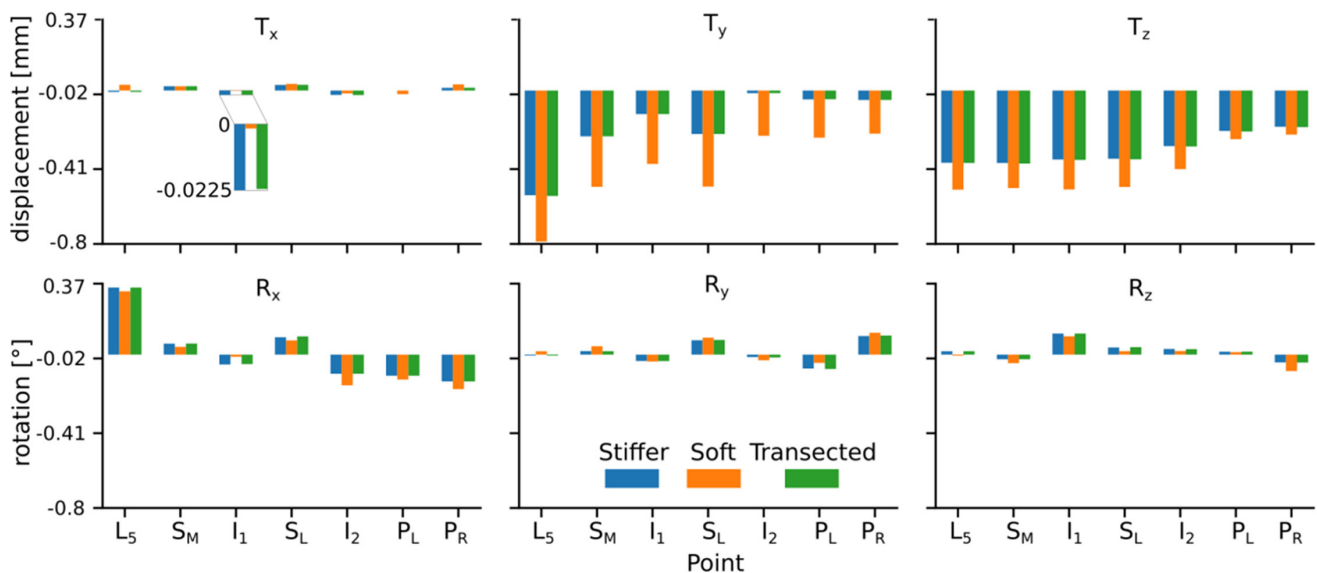

FIGURE 5 Absolute variations of displacements in (mm) and rotations in (°) for monitored locations under three scenarios "Stiffer state", "Soft state," and "Transected state", respectively. Owing to the small extent in T_x in spite of the vast 1393% change in relative movement, T_x is further magnified (insert) to enhance readability.

value of −0.01 millidegree/N was found for point L_5 around the axis-z.

3.3 | Relative deformation sensitivity

The highest sensitivity value −0.57 μm/N was found for the relative displacement of pair L_5-S_M in the direction of axis-y, while the lowest value found of −0.01 μm/N for a pair P_L-I_2 in the direction of axis-x. The highest rotation sensitivity value, 0.58 millidegree/N, was found for a pair L_5-S_M around the axis-x, while the lowest value −0.01 millidegree/N was found for a pair P_L-I_2 around the axis-z; as shown in Figure 4.

3.4 | Absolute deformation evaluation

3.4.1 | The difference in displacements/rotations between "Stiffer state" and "Soft state"

The displacement T_x of point P_L and displacement T_y of point I_2 were significantly higher in the "Soft state" than in the "Stiffer state" (1598%). The displacement T_x of point S_M was found to be insensitive to changes in ligament properties (0.4%). The most significant change in rotation was found for point L_5 around the axis-y (468%), while the lowest value was found for point L_5 around the axis-x (5.7%) (see Figure 5).

3.4.2 | The difference in displacements/rotations between "Soft state" and "Transected state"

The most significant difference between the soft and transected states was found for displacement T_x of point I_1 (1393%), while the lowest value 1.8% was found for point S_M in displacement T_x. Point L5 was found to be most sensitive in rotation around the axis-x (434%). Point I_1 was almost insensitive around axis-y (6.1%) (see Figure 5).

3.4.3 | The difference in displacements/rotations between "Stiffer state" and "Transected state"

The most significant difference in displacements between the stiffer and transected states was found in point P_L in the direction of axis-x (3.4%), while the lowest value (0.01%) was found for points S_M, I_1 and S_L in the direction of axis-y. The most sensitive rotation was found in point I_2 around the axis-y (14.7%) (see Figure 5).

3.5 | Evaluation of relative deformation

3.5.1 | The difference in displacements/rotations between "Stiffer state" and "Soft state"

The highest difference in displacement was found for pair L_5-S_M with a value of 900% in the direction of axis-z. The lowest difference was found for pair L_5-S_M with 6.8% in the direction of axis-y. The most evident difference in rotation was found for pair P_L-I_2 with a difference of 400% around the axis-x. The lowest difference was found for pair L_5-S_M with a value of 1.2% around the axis-y (see Figure 6).

3.5.2 | The difference in displacements/rotations between "Soft state" and "Transected state"

The relative displacement of pair P_L-I_2 is the most different (721%) between the soft and transected states in the direction of axis-x, while the T_z displacement of pair P_R-P_L stays nearly insensitive (4.2%). The most significant difference (353%) in rotation was found for pair P_L-I_2 around the axis-y. The lowest difference in rotation was found for the pair L_5-S_M around the axis -x (1%) (see Figure 6).

3.5.3 | The difference in displacements/rotations between "Stiffer state" and "Transected state"

The most significant difference in displacement between stiffer and transected states was found in L_5-S_M (200%) in the direction of axis-z, while the lowest value was found in I_1-S_L (0.1%) in the direction of axis-y. The difference in rotation was low (max. 2.9%) for all pairs (see Figure 6).

4 | DISCUSSION

Surgical transection of the SS and ST is performed in therapy-resistant cases of pudendal nerve entrapment where non-operative treatment options fail (Bollens et al., 2021; Loukas et al., 2006; Philippeau et al., 2008; Ploteau et al., 2016; Robert et al., 1998). Similarly, the ligaments may fail or be injured in cases of pelvic injury (Böhme et al., 2014; Hammer et al., 2013) or in rare cases of hamstring tears (Bierry et al., 2014). It is unclear if partial to full failure of the SS and ST may cause the pelvis to destabilize, though previous numerical (Böhme et al., 2014; Hammer et al., 2013;
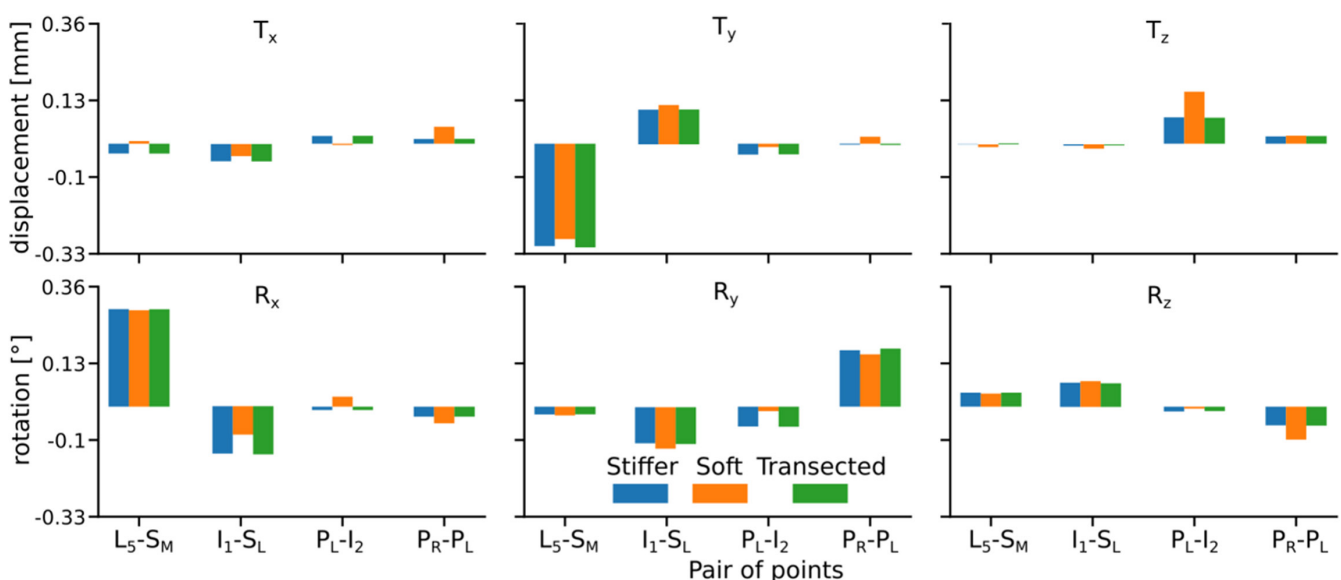

FIGURE 6 The relative variations of displacement in (mm) and rotation in (°) for pairs of monitored locations under three scenarios "Stiffer state", "Soft state", and "Transected state", respectively.

Toyohara et al., 2020) and biomechanical (Steinke et al., 2014) studies provided the first evidence of severe alterations to the minute movements of the sacroiliac joint (SIJ) under physiological loading following ligament injury. More refined experimental models are needed to understand the consequences of SS and ST insufficiency related to surgical intervention or ligament rupture in detail. However, to date, even the mechanical properties of the SS and STS are poorly investigated, owing to the lacking methodology to elucidate stress–strain values of polyaxial, anisotropic ligaments with their highly complex geometries.

The influence of the SS and ST ligament on pelvis kinematics has been assessed, deploying a numerical model based on the FE method (Hammer, Scholze, et al., 2019; Ramezani et al., 2019). The model included fine detail fiber orientations of all pelvic ligaments and the hip joint (Pieroh et al., 2016; Schleifenbaum et al., 2016) and experimentally obtained load-deformation data of the SS and ST from human cadavers (Hülse et al., 2009). The following hypotheses were addressed:

An experimental validation of the cadaveric pelvises yielded congruency of the numerical and cadaveric results (hypothesis A), especially for the translations (Hammer & Klima, 2019; Hammer, Scholze, et al., 2019; Klima et al., 2018). Some outliers were found for the rotations, especially where minute (non-significant) rotations were seen, which is likely related to measurement inaccuracies in the image correlation of the validation experiments, or to interindividual variation of donors.

Based on the results of this study, hypothesis (B) must be rejected. The reasoning behind the observed phenomena remains unclear and warrants further in-depth research including cadaveric analyses. Nevertheless, alterations in SS and ST mechanical properties compared to an initial state ("Stiffer" vs. "Soft") cause changed load response of the SIJ, lumbosacral transition, and hip joints. The computer model used in this study is augmented with the actual geometry of the femoral bone. An objective representation of the bone geometry is important for accurate estimation of deformation and stress in the pelvis and provides better estimation of stiffness than previous models (Böhme et al., 2014; Hammer et al., 2013).

4.1 | Pelvis kinematics with stiffer SS and ST seem similar to pelvis kinematics with transected ligaments

This given numerical model showed that lowered S and SS stiffness ("Soft state") resulted in larger alterations in translations than a complete transection of the ligaments ("Transected state"). This trend was observed consistently, especially in T_y and T_z. Vice versa, the state with the fully released SS and ST ($E = 0$ MPa; "Transected state") yielded similar and consistent load deformation results as compared to the stiffer state of the SS and ST ($E = 25$ MPa; "Stiffer state"). Notwithstanding these observations, absolute movements were in the range of micrometers and millidegrees, which underlines the relevance even of such small movements at the posterior pelvis.

The similarity between the stiffer and transected models may be explained as follows. The applied load is symmetrical and causes mainly deformations in the T_y and T_z axes and rotation about the R_x axis. The positive rotation at L_5 indicates that the ST/SS ligaments are loaded in tension and therefore affect the magnitude of the rotation about R_x and, of course, the deformations in the T_y and T_z axes. Although the ligaments on the left side are absent in the transected model, their function may be replaced by the ligaments contralateral to some extent. The soft model must be differentiated from both other test variables because it considers different properties of the ligaments on the two sides. The difference between the stiff and transected models would probably stand out if loads had to be considered that are not symmetrical. This explanation, however, warrants further investigation to provide further insight into the observations.

4.2 | Relative changes in pelvis kinematics related to SS and ST stiffness were seen at the lumbosacral transition and within the innominate bone

Similar to the absolute deformations observed in the numerical model, relative changes in load deformation were strongly site dependent. Considering the changes, mobility alterations were observed at the lumbosacral junction in T_y and R_x. Moreover, vast relative (but minute absolute) changes were seen at the site of the innominate bones and the pubic symphysis. As one outstanding observation, lowered SS and ST stiffness resulted in increased innominate bone (T_y) mobility. These results are in line with our previous numerical experiments on the pelvis (Hammer, Scholze, et al., 2019; Ramezani et al., 2019), considering the alterations introduced by the new material properties for the SS and ST.

4.3 | SS and ST stiffness seem to influence the extent and direction of movements at the lumbosacral transition and within the innominate bone—an underappreciated role of the ligament complex?

In line with the observations made for absolute values, the transected condition seemed to result in similar movements as the stiffer condition. Vice versa, altering movements were observed when more realistic (accurate) ligament properties were modeled ("Soft state"). These results indicate that the SS and ST indeed play an integral role in redirecting load distributions at the human pelvis. One may hypothesize that consecutive symptoms resulting from pudendal nerve release may be similar to those symptoms resulting from overly stiff ligaments. Ligament stiffness (Hammer, Ondruschka, et al., 2019; Poilliot et al., 2019) has been hypothesized besides ligament laxity as one of the factors causing SIJ dysfunction or pain (Arumugam et al., 2012; Cusi et al., 2013; Mens et al., 1999).

4.4 | Revisiting pelvis biomechanics as a coupled system of the hip–spine complex

The SIJ is embedded within a closely coupled system of bone segments connected vertically and horizontally, thereby coupling the lumbar spine with the lower limbs and the pelvic ring. Superiorly, the SIJ is connected with the lumbosacral transition and inferiorly with both hip joints. Horizontally, the SIJs are coupled with their contralateral counterpart and anteriorly with the pubic symphysis. The SIJ sits centrally within this highly complex kinematic chain. It serves to provide stability on one side, while on the other side, it provides sufficient elasticity to dissipate load peaks occurring under the activities of daily life. For this purpose, the SIJ has a number of unique morphological features: It consists anteriorly of a diarthrotic (synovial) part, while the posterior region of the SIJ comprises dense fiber bundles aligned in various directions. The observable movements in the SIJ are minimal but existent. Therefore, the SIJ sits between two regions where disease of the musculoskeletal apparatus may become symptomatic—the lumbar spine and the hip joints (Bitton, 2009). Pain originating from the SIJ has been described in up to 30% of the low back pain population (Cohen et al., 2013; Forst et al., 2006; Fortin, 1993; Fortin et al., 1999; Szadek et al., 2009; Visser et al., 2013). SIJ pain is hypothesized to be a consequence of trauma (Cohen et al., 2013; Vleeming et al., 2012), surgery, pregnancy, and old age (Cohen et al., 2013; Laplante et al., 2012), but is also related to increased SIJ laxity (Arumugam et al., 2012; Cusi et al., 2013; Mens et al., 2006).

With no doubt, the SIJ compensates for pathologies resulting in altered posture of the lumbar spine or hip joint. Local mechanical properties attributed to the various ligaments, cartilage, and (sub-chondral) bone properties may form a reciprocal relationship, decisive for overall motion and stress concentration at the lumbosacrum, pelvic ring, and hip joints. Two ligaments are situated posterior-inferiorly at the pelvis—the SS and ST ligaments. These are involved in load dissipation of the SIJ and may be decisive for the transmission in which the pelvis is involved between the lumbar spine and the hip joint. Alterations in ligament properties may relate to changed pelvis deformation, and this may also have effects on the lumbar spine and hip joint.

4.5 | Experimental models on pelvic trauma are potentially unsuitable to assess the mechanical effects of SIJ pathology and therapeutic interventions

Previous biomechanical experiments with focus on the posterior pelvis were so far largely limited to pelvic disruption, in particular on types B and C pelvic ring injury (Doro et al., 2010; Golden et al., 2013; Hefzy et al., 2003; McLachlin et al., 2018) and the consequence of surgical treatment on pelvic stability (Abdelfattah & Moed, 2014; Dienstknecht et al., 2011; Giraldez-Sanchez

et al., 2015; Queipo-de-Llano et al., 2013). So far, very few studies have focused on the consequences of isolated posterior ligament insufficiency (Philippeau et al., 2008; Vrahas et al., 1995; Vukicevic et al., 1991) in cadaveric models and yielded controversial results. Ligament insufficiency, "incompetence" (Cusi et al., 2013), or "slackening" (Vleeming et al., 1992) has repeatedly been reported in relation to SIJ pain and was therefore the rationale for the model proposed here. The study on pelvic ligaments by Vleeming et al. (1989) found that transection does alter SIJ nutation, which can be approved by the given results of this study. Vukicevic et al. (1991), Vrahas et al. (1995) and Wang and Dumas (1998) also found that ligament injury has site-dependent impact on pelvic stability, and that the pubic symphysis does act as the main contributor to pelvic stability. These general findings can be confirmed by the given experiments in a physiologic loading scenario, however with absolute movements in the SIJ being much smaller than reported previously using FE simulation. The given results are furthermore in line with numerical analyses on pelvic motion, indicating that ligament stiffness may alter load deformation (Eichenseer et al., 2011; Hammer et al., 2013).

4.6 | Study limitations

The used computational model lacks a detailed material model of bone. The bone properties were set being constant over the bone, but are known to vary significantly with bone mineral density (Henys et al., 2021). Another limitation can be seen in boundary conditions representing accurately anatomical conditions, which is difficult to achieve. Both these limitations contribute to model inaccuracy obtained. The divergence in results is seen mainly in rotations. Due to minute values of rotations, the accuracy of the experimental method can also be disputable (Hammer, Scholze, et al., 2019), and hence, the computational and experimental rotation results must be carefully interpreted. The effect of FE model parameters and their estimation could be further improved by using more sophisticated methods such as Design of Experiment, which was effectively used in (Somovilla-Gomez et al., 2020) to analyze the effect of age and gender on the relative motion of the functional spinal unit. The interaction between the bones was approximated by a bond that does not allow relative motion. This type of contact does not represent the actual mobility in the joint, and in the next generation FE model, an interaction allowing to simulate a fully mobile joint will be introduced (Lostado Lorza et al., 2021).

5 | CONCLUSIONS AND CLINICAL IMPLICATIONS

Alterations in SS and ST ligament stiffness have substantial influence on pelvis kinematics. This influence appears nonlinear. The findings further suggest that a certain prestrain exists for the SS and ST.

Transection of the ligaments is related to alterations in particular at the lumbosacral transition and within the innominate bone.

AUTHOR CONTRIBUTIONS

Contributions to concept/design: MR, NH; acquisition of data: PH, MR, DS; data analysis/interpretation: all authors; drafting of the manuscript: PH, MR, BO, NH; critical revision of the manuscript and approval of the article: all authors.

DATA AVAILABILITY STATEMENT

Data will be made available upon reasonable request.

ORCID

Petr Henyš https://orcid.org/0000-0002-8700-0163
Niels Hammer https://orcid.org/0000-0001-8230-9383

REFERENCES

Abdelfattah, A. & Moed, B.R. (2014) Ligamentous contributions to pelvic stability in a rotationally unstable open-book injury: a cadaver study. *Injury*, 45, 1599–1603.

Aldabe, D., Hammer, N., Flack, N. & Woodley, S.J. (2019) A systematic review of the morphology and function of the sacrotuberous ligament. *Clinical Anatomy*, 32, 396–407.

Arumugam, A., Milosavljevic, S., Woodley, S. & Sole, G. (2012) Effects of external pelvic compression on form closure, force closure, and neuromotor control of the lumbopelvic spine—a systematic review. *Manual Therapy*, 17, 275–284.

Bierry, G., Simeone, F.J., Borg-Stein, J.P., Clavert, P. & Palmer, W.E. (2014) Sacrotuberous ligament: relationship to normal, torn, and retracted hamstring tendons on MR images. *Radiology*, 271, 162–171.

Bitton, R. (2009) The economic burden of osteoarthritis. *The American Journal of Managed Care*, 15, S230–S235.

Böhme, J., Lingslebe, U., Steinke, H., Werner, M., Slowik, V., Josten, C. et al. (2014) The extent of ligament injury and its influence on pelvic stability following type II anteroposterior compression pelvic injuries—a computer study to gain insight into open book trauma. *Journal of Orthopaedic Research*, 32, 873–879.

Böhme, J., Steinke, H., Huelse, R., Hammer, N., Klink, T., Slowik, V. et al. (2011) [Complex ligament instabilities after "open book"-fractures of the pelvic ring—finite element computer simulation and crack simulation]. *Zeitschrift für Orthopädie und Unfallchirurgie*, 149, 83–89.

Bollens, R., Mjaess, G., Sarkis, J., Chemaly, A.K., Nemr, E., Daher, K. et al. (2021) Laparoscopic transperitoneal pudendal nerve and artery release for pudendal entrapment syndrome. *Surgical Endoscopy*, 35, 6031–6038.

Cohen, S.P., Chen, Y. & Neufeld, N.J. (2013) Sacroiliac joint pain: a comprehensive review of epidemiology, diagnosis and treatment. *Expert Review of Neurotherapeutics*, 13, 99–116.

Cusi, M., Saunders, J., Van der Wall, H. & Fogelman, I. (2013) Metabolic disturbances identified by SPECT-CT in patients with a clinical diagnosis of sacroiliac joint incompetence. *European Spine Journal*, 22, 1674–1682.

De Decker, A., Fergusson, R., Ondruschka, B., Hammer, N. & Zwirner, J. (2020) Anatomical structures at risk using different approaches for sacrospinous ligament fixation. *Clinical Anatomy*, 33, 522–529.

Dienstknecht, T., Berner, A., Lenich, A., Zellner, J., Mueller, M., Nerlich, M. et al. (2011) Biomechanical analysis of a transiliac internal fixator. *International Orthopaedics*, 35, 1863–1868.

Doro, C.J., Forward, D.P., Kim, H., Nascone, J.W., Sciadini, M.F., Hsieh, A.H. et al. (2010) Does 2.5 cm of symphyseal widening differentiate anteroposterior compression I from anteroposterior compression II pelvic ring injuries? *Journal of Orthopaedic Trauma*, 24, 610–615.

Eichenseer, P.H., Sybert, D.R. & Cotton, J.R. (2011) A finite element analysis of sacroiliac joint ligaments in response to different loading conditions. *Spine*, 36, E1446–E1452.

Fick, R.A. (1904) *Handbuch Der Anatomie Und Mechanik Der Gelenke Unter Bercksichtigung Der Bewegenden Muskeln*. Jena: Gustav Fischer.

Forst, S.L., Wheeler, M.T., Fortin, J.D. & Vilensky, J.A. (2006) The sacroiliac joint: anatomy, physiology and clinical significance. *Pain Physician*, 9, 61–67.

Fortin, J.D. (1993) Sacroiliac joint dysfunctiona new perspective. *Journal of Back and Musculoskeletal Rehabilitation*, 3, 31–43.

Fortin, J.D., Kissling, R.O., O'Connor, B.L. & Vilensky, J.A. (1999) Sacroiliac joint innervation and pain. *American Journal of Orthopedics*, 28, 687–690.

Giráldez-Sanchez, M.A., Lázaro-Gonzálvez, A., Martinez-Reina, J., Serrano-Toledano, D., Navarro-Robles, A., Cano-Luis, P. et al. (2015) Percutaneous iliosacral fixation in external rotational pelvic fractures. A biomechanical analysis. *Injury*, 46, 327–332.

Golden, R.D., Kim, H., Watson, J.D., Oliphant, B.W., Doro, C., Hsieh, A.H. et al. (2013) How much vertical displacement of the symphysis indicates instability after pelvic injury? *Journal of Trauma and Acute Care Surgery*, 74, 585–589.

Hammer, N. & Klima, S. (2019) In-silico pelvis and sacroiliac joint motion—a review on published research using numerical analyses. *Clinical Biomechanics*, 61, 95–104.

Hammer, N., Ondruschka, B. & Fuchs, V. (2019) Sacroiliac joint ligaments and sacroiliac pain: a case-control study on micro- and ultrastructural findings on morphologic alterations. *Pain Physician*, 22, E615–E625.

Hammer, N., Scholze, M., Kibsgård, T., Klima, S., Schleifenbaum, S., Seidel, T. et al. (2019) Physiological in vitro sacroiliac joint motion: a study on three-dimensional posterior pelvic ring kinematics. *Journal of Anatomy*, 234, 346–358.

Hammer, N., Steinke, H., Lingslebe, U., Bechmann, I., Josten, C., Slowik, V. et al. (2013) Ligamentous influence in pelvic load distribution. *The Spine Journal*, 13, 1321–1330.

Hammer, N., Steinke, H., Slowik, V., Josten, C., Stadler, J., Böhme, J. et al. (2009) The sacrotuberous and the sacrospinous ligament—a virtual reconstruction. *Annals of Anatomy*, 191, 417–425.

Hayashi, S., Kim, J.H., Rodriguez-Vazquez, J.F., Murakami, G., Fukuzawa, Y., Asamoto, K. et al. (2013) Influence of developing ligaments on the muscles in contact with them: a study of the annular ligament of the radius and the sacrospinous ligament in mid-term human fetuses. *Anatomy & Cell Biology*, 46, 149–156.

Hefzy, M.S., Ebraheim, N., Mekhail, A., Caruntu, D., Lin, H. & Yeasting, R. (2003) Kinematics of the human pelvis following open book injury. *Medical Engineering & Physics*, 25, 259–274.

Henyš, P., Vorechovsky, M., Kucha, M., Heinemann, A., Kopal, J., Ondruschka, B. et al. (2021) Bone mineral density modeling via random field: normality, stationarity, sex and age dependence. *Computer Methods and Programs in Biomedicine*, 210, 106353.

Hülse, R., Hammer, N., Steinke, H., Stadler, J., Hülse, K., Slowik, V. et al. (2009) Finite Elemente Modell des Beckens zur Simulation komplexer ligamentärer Instabilitätsszenarien. In: Meinzer, H.P., Deserno, T.M., Handels, H. & Tolxdorff, T. (Eds.) *Bildverarbeitung für die Medizin 2009*. Berlin, New York: Springer, pp. 434–438.

Kaur, J. & Singh, P. (2022) *Pudendal nerve entrapment syndrome*. Treasure Island, FL: StatPearls.

Klima, S., Grunert, R., Ondruschka, B., Scholze, M., Seidel, T., Werner, M. et al. (2018) Pelvic orthosis effects on posterior pelvis kinematics an in-vitro biomechanical study. *Scientific Reports*, 8, 15980.

Laplante, B.L., Ketchum, J.M., Saullo, T.R. & DePalma, M.J. (2012) Multivariable analysis of the relationship between pain referral

patterns and the source of chronic low back pain. *Pain Physician*, 15, 171–178.

Lostado-Lorza, R., Somovilla-Gómez, F., Corral Bobadilla, M., Íñiguez Macedo, S., Rodríguez San Miguel, A., Fernández Martínez, E. et al. (2021) Comparative analysis of healthy and cam-type femoroacetabular impingement (FAI) human hip joints using the finite element method. *Applied Sciences*, 11, 11101.

Loukas, M., Louis, R.G., Jr., Hallner, B., Gupta, A.A. & White, D. (2006) Anatomical and surgical considerations of the sacrotuberous ligament and its relevance in pudendal nerve entrapment syndrome. *Surgical and Radiologic Anatomy*, 28, 163–169.

McLachlin, S., Lesieur, M., Stephen, D., Kreder, H. & Whyne, C. (2018) Biomechanical analysis of anterior ring fixation of the ramus in type C pelvis fractures. *European Journal of Trauma and Emergency Surgery*, 44, 185–190.

Mens, J.M., Damen, L., Snijders, C.J. & Stam, H.J. (2006) The mechanical effect of a pelvic belt in patients with pregnancy-related pelvic pain. *Clinical Biomechanics*, 21, 122–127.

Mens, J.M., Vleeming, A., Snijders, C.J., Stam, H.J. & Ginai, A.Z. (1999) The active straight leg raising test and mobility of the pelvic joints. *European Spine Journal*, 8, 468–473.

Philippeau, J.M., Hamel, O., Pecot, J. & Robert, R. (2008) [Are sacrospinal and sacrotuberal ligaments involved in sacro-iliac joint stability?] *Morphologie*, 92, 16–30.

Pieroh, P., Schneider, S., Lingslebe, U., Sichting, F., Wolfskämpf, T., Josten, C. et al. (2016) The stress-strain data of the hip capsule ligaments are gender and side independent suggesting a smaller contribution to passive stiffness. *PLoS One*, 11, e0163306.

Ploteau, S., Cardaillac, C., Perrouin-Verbe, M.A., Riant, T. & Labat, J.J. (2016) Pudendal neuralgia due to pudendal nerve entrapment: warning signs observed in two cases and review of the literature. *Pain Physician*, 19, E449–E454.

Poilliot, A.J., Zwirner, J., Doyle, T. & Hammer, N. (2019) A systematic review of the normal sacroiliac joint anatomy and adjacent tissues for pain physicians. *Pain Physician*, 22, E247–E274.

Queipo-de-Llano, A., Perez-Blanca, A., Ezquerro, F. & Luna-González, F. (2013) Simultaneous anterior and posterior compression of the pelvic ring with external fixation using a pre-tensed curved bar: a biomechanical study. *Injury*, 44, 1787–1792.

Ramezani, M., Klima, S., de la Herverie, P.L.C., Campo, J., Le Joncour, J.B., Rouquette, C. et al. (2019) In silico pelvis and sacroiliac joint motion: refining a model of the human osteoligamentous pelvis for assessing physiological load deformation using an inverted validation approach. *BioMed Research International*, 2019, 3973170.

Robert, R., Prat-Pradal, D., Labat, J.J., Bensignor, M., Raoul, S., Rebai, R. et al. (1998) Anatomic basis of chronic perineal pain: role of the pudendal nerve. *Surgical and Radiologic Anatomy*, 20, 93–98.

Schleifenbaum, S., Prietzel, T., Hädrich, C., Möbius, R., Sichting, F. & Hammer, N. (2016) Tensile properties of the hip joint ligaments are largely variable and age-dependent—an in-vitro analysis in an age range of 14–93 years. *Journal of Biomechanics*, 49, 3437–3443.

Sichting, F., Rossol, J., Soisson, O., Klima, S., Milani, T. & Hammer, N. (2014) Pelvic belt effects on sacroiliac joint ligaments: a computational approach to understand therapeutic effects of pelvic belts. *Pain Physician*, 17, 43–51.

Somovilla-Gómez, F., Lostado-Lorza, R., Corral-Bobadilla, M. & Escribano-Garcia, R. (2020) Improvement in determining the risk of damage to the human lumbar functional spinal unit considering age, height, weight and sex using a combination of FEM and RSM. *Biomechanics and Modeling in Mechanobiology*, 19, 351–387.

Steinke, H., Hammer, N., Lingslebe, U., Höch, A., Klink, T. & Böhme, J. (2014) Ligament-induced sacral fractures of the pelvis are possible. *Clinical Anatomy*, 27, 770–777.

Szadek, K.M., van der Wurff, P., van Tulder, M.W., Zuurmond, W.W. & Perez, R.S. (2009) Diagnostic validity of criteria for sacroiliac joint pain: a systematic review. *The Journal of Pain*, 10, 354–368.

Toyohara, R., Kurosawa, D., Hammer, N., Werner, M., Honda, K., Sekiguchi, Y. et al. (2020) Finite element analysis of load transition on sacroiliac joint during bipedal walking. *Scientific Reports*, 10, 13683.

Venayre, B., Koyama, Y., Kurosawa, D., Hammer, N., Lingslebe, U., Murakami, E. et al. (2021) Quantitative evaluation of the sacroiliac joint fixation in stress reduction on both sacroiliac joint cartilage and ligaments: a finite element analysis. *Clinical Biomechanics*, 85, 105350.

Visser, L.H., Nijssen, P.G., Tijssen, C.C., van Middendorp, J.J. & Schieving, J. (2013) Sciatica-like symptoms and the sacroiliac joint: clinical features and differential diagnosis. *European Spine Journal*, 22, 1657–1664.

Vleeming, A., Schuenke, M.D., Masi, A.T., Carreiro, J.E., Danneels, L. & Willard, F.H. (2012) The sacroiliac joint: an overview of its anatomy, function and potential clinical implications. *Journal of Anatomy*, 221, 537–567.

Vleeming, A., Stoeckart, R. & Snijders, C.J. (1989) The sacrotuberous ligament; a conceptual approach to its dynamic role in stabilizing the sacroiliac joint. *Clinical Biomechanics*, 4, 201–203.

Vleeming, A., Van Wingerden, J.P., Dijkstra, P.F., Stoeckart, R., Snijders, C.J. & Stijnen, T. (1992) Mobility in the sacroiliac joints in the elderly: a kinematic and radiological study. *Clinical Biomechanics*, 7, 170–176.

Vrahas, M., Hern, T.C., Diangelo, D., Kellam, J. & Tile, M. (1995) Ligamentous contributions to pelvic stability. *Orthopedics*, 18, 271–274.

Vukicević, S., Marusić, A., Stavljenic, A., Vujicic, G., Skavić, J. & Vukicević, D. (1991) Holographic analysis of the human pelvis. *Spine*, 16, 209–214.

Wang, M. & Dumas, G.A. (1998) Mechanical behavior of the female sacroiliac joint and influence of the anterior and posterior sacroiliac ligaments under sagittal loads. *Clinical Biomechanics*, 13, 293–299.